

Deep IRLS Net: DNN-based Localization with Efficient Ray Tracing-Free Simulation

Tetsuro Sato¹, Hiroyuki Kamata¹, Takahiro Tsujii¹, Kenei Matsudaira¹ and Kosei Yamashita¹

¹Technology Development Laboratories, Sony Corporation, Tokyo, Japan

Abstract

In this paper, we have achieved positioning performance exceeding the conventional method Weighted Least Squares (WLS) by applying DNN-based IRLS Net to the indoor environment with multipath effects including non-line-of-sight (NLOS) signals. Among types of positioning, indoor environments in which signal shielding and reflection occur frequently are environments where high-precision positioning is difficult to achieve. We propose 1) IRLS Net, a DNN model that takes its inspiration from Iteratively Reweighted Least Squares (IRLS), and 2) a learning method that uses a simple ray tracing-free simulation to effectively train this network. The proposed method encompasses general positioning methods such as the Time Difference of Arrival (TDOA), and can be applied to conventional positioning technologies such as Ultra-Wide Band (UWB). The IRLS Net has a deep neural network (DNN) structure in which the internal state is updated iteratively to reduce the influence of observed values with large errors due to multipath and NLOS. When training a deep network structure, data collected in various environments is required to avoid overfitting and achieve sufficient generalization performance. However, it is not easy to collect actual environment data that encompasses many different indoor environments. It is possible to use ray tracing to simulate signal reflection and shielding for training data, but preparing a 3D map for each actual environment is also difficult. Our ray tracing-free simulation focuses on the fact that the multipath and NLOS effects are compressed into one-dimensional errors at pseudo-distances in the TDOA information that is preprocessed until the pseudo-distance from the arrival time is calculated. IRLS Net learned only using the data created through the proposed ray tracing-free simulation and evaluated it using real acoustic positioning data. As a result, we confirmed that IRLS Net sufficiently generalized the measured data and report that the result exceeded WLS, which was the baseline for comparison.

Keywords

DNN, TDOA, IRLS, ray tracing-free

1. Introduction


Indoor positioning is becoming increasingly important and plays important roles in areas such as indoor navigation, smart homes and IoT. Positioning methods include TDOA, TOA (Time of Arrival), and TWR (Two-Way Ranging), which utilize the arrival time of radio waves or acoustic signals, as well as methods that use RSSI (received signal strength) from Wi-Fi access points and BT beacons. In TDOA, anchors transmit radio waves or acoustic signals to tags to measure

Proceedings of the Work-in-Progress Papers at the 13th International Conference on Indoor Positioning and Indoor Navigation (IPIN-WiP 2023), September 25 - 28, 2023, Nuremberg, Germany

✉ Tetsuro.Sato@sony.com (T. Sato); Hiroyuki.Kamata@sony.com (H. Kamata); Takahiro.Tsujii@sony.com (T. Tsujii); Kenei.Matsudaira@sony.com (K. Matsudaira); Kosei.Yamashita@sony.com (K. Yamashita)



© 2023 Copyright for this paper by its authors. Use permitted under Creative Commons License Attribution 4.0 International (CC BY 4.0).

 CEUR Workshop Proceedings (CEUR-WS.org)

the signal arrival time. When there is no time synchronization between the anchors and tags, a clock error is added to the arrival times of each anchor. Therefore, the difference in arrival times between each anchor is used to remove the clock error and to calculate the tag position. This method is used in GNSS [1] and can be used to estimate positions with high accuracy without complex communication between anchors and tags.

Multipath and NLOS (Non-Line-of-Sight) are significant problems in TDOA positioning. Accurate measurement of the signal arrival time greatly affects positioning accuracy, making it important to secure a direct communication path. The insides of buildings are enclosed spaces and are environments where a variety of items are placed. Their walls, ceilings and other obstacles directly block waves and pick up reflections, meaning that arrival times are measured differently from actual direct paths, leading to large positioning errors. [2] Several methods such as IRLS (Iteratively Reweighted Least Squares) that optimizes positioning by receiving signals from a redundant number of anchors and reducing the effect of anchors that pick up reflected paths other than direct paths [3], and methods that estimates the anchors affected by NLOS and removes them from the anchors used for positioning [4][5][6] have been proposed to reduce the impact of these problems. In this study, we propose a novel DNN model for solving the problems with multipath and NLOS, and in which learning is performed by generating training data using ray tracing-free simulation. This paper makes the following two contributions to research on this subject.

- IRLS Net: We report that we have obtained results from this model inspired by IRLS that are better than with WLS.
- Ray tracing-free simulation: We demonstrate that the model trained on data generated by this method can generalize to data in the real environment.

In this study, experiments were conducted using acoustic positioning on real environment data. The proposed DNN model and simulation method can be applied to other positioning technologies, such as UWB.

2. Related work

It has been reported that highly precise positioning is possible using IRLS. [3] However, robustness is insufficient in environments that are greatly affected by multipaths. Here, multiple studies that apply deep learning to positioning exist, and it has been reported that they demonstrate high performance. Application of deep learning to GNSS positioning has been proposed. In [7], a transformer with a structure that does not depend on the order of the observed satellites is used. Because signals cannot always be received in a fixed order during TDOA positioning, it is important to have an invariant structure in the order of observations. In our proposed method, we were able to achieve similar functions with a structure that used simpler average pooling.

Other examples of applying deep learning to fingerprinting using RSS [8][9], and examples of applying deep learning to positioning using UWB [10][11] in indoor environments have been reported. In [8] and [9], a Deep Belief Network with multiple fully connected layers is used for inference, while in [12], a convolutional neural network is used. In [10] and [11], a

network structure that maintains time-series information such as LSTM is used, and accuracy is improved by repeating inferences in the time direction. Although time-series information is not used in our proposal, it has a structure in which iterative multiple position estimation is performed and in which estimation accuracy is improved.

These previous studies have used real environment data as training data, or are only simulations of training and evaluation. Because applying a method to diverse real environments requires a great deal of time for collecting various real environment data, several proposals have been made to reduce the difficulty of collecting real environment data. In [13], a proposal is made to improve robustness by augmenting real RSS data by changing random values to machine learning methods for indoor positioning technology. In [14], pseudo data is created from real data using a generative adversarial network. Although it has been shown that estimation accuracy can be improved by adding training data, real data is still required for data augmentation.

In [15], in order to reduce microphone noise and TDOA error between microphones, the study trains with simulation data using an impulse generation model and verifying it with real data. However, this study focuses on detecting arrival times from signals. Our method proposes a method of positioning that improves position accuracy in real environments by generating simulation data that considers TDOA errors in multipath and NLOS environments. In [16], learning is performed by acquiring LOS, NLOS, and multipath labels via ray tracing using 3D maps. It requires preparing a 3D map of the target environment. In [17], CIR fingerprints using ray tracing are used for training. To reduce the difficulty of making a fingerprint again when a real environment has changed significantly, [18] proposes pre-training with CSI information created in the simulation and transfer learning with a small number of data collected in the real environment. These proposals are only effective if the real environment where the positioning will be used is predetermined. In our method, training is performed using only simulation data while verification is performed in the real environment. The ray tracing is not used and it is not limited to a specific environment. Our proposed DNN model trained by our ray tracing-free simulation operate in various environments without prior preparation.

3. Our method

Section 3 describes how we created simulation data and how the training model works.

3.1. Data generation using ray tracing-free simulation

In the basis of TDOA positioning, tags that receive signals transmitted by multiple anchors obtain pseudo-distances by measuring the time until the signal arrives. The three-dimensional positions of the tags are calculated from the pseudo-distances of four or more anchors. The main causes of errors that reduce the accuracy of TDOA positioning are observation errors, multipath errors due to reflection effects, and NLOS errors due to shielding effects. These errors must be taken into account in the training data so that the machine learning model is to make robust estimates even in a real environment that includes these errors. In particular, errors derived from multipath and NLOS vary greatly according to the environment. When collecting data that includes multipath and NLOS in a real environment, it is necessary to acquire data in

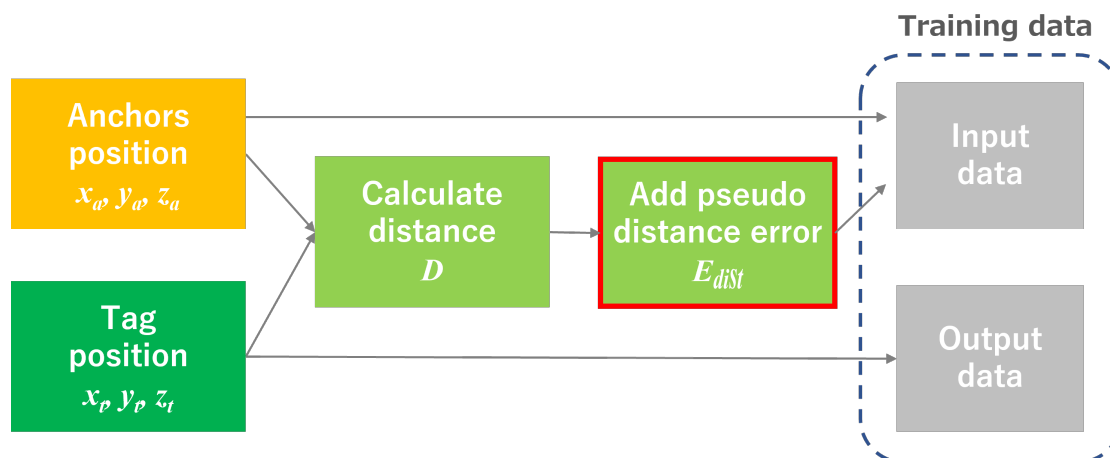


Figure 1: Overview of our ray tracing-free simulation

many different indoor environments. In addition, when using ray tracing to precisely simulate the kind of path that was followed from an anchor to a tag, including reflection and shielding, it is necessary to have 3D maps for each environment to be simulated and to operate under computationally expensive.

In this proposal, simulation data is generated for indoor TDOA positioning, but ray tracing is not used. The generated artificial data is related to the pseudo-distances obtained from preprocessed signals and is not a simulation of the signal itself. The pseudo-distance is one-dimensional information that represents the distance between an anchor and a tag. The effects of multipath and NLOS are also compressed into one-dimensional information, eliminating the need to know exactly what path the signal emitted from the anchor took to reach the tag. For example, even if a signal emitted from an anchor reaches a tag after being reflected off the ceiling or off a side wall, if they have similar distance errors, there is no need to distinguish the difference between the two errors in terms of pseudo-distance. Therefore, it is not necessary to prepare precise reflection paths by ray tracing, and it is assumed that errors due to the effects of multipath and NLOS can be simulated with some extremely simple equations. Assuming that these error factors occur with a certain probability, pseudo-distance errors E_{dist} are formulated as follows.

$$E_{obs} = \text{Bernoulli}(p_{obs}) \times \text{Uniform}(a_{obs}, b_{obs}) \quad (1)$$

$$E_{env} = \text{Bernoulli}(p_{env}) \times \text{Uniform}(a_{env}, b_{env}) \quad (2)$$

$$E_{dist} = E_{obs} + E_{env} \quad (3)$$

Here, observation errors are shown as E_{obs} , while multipath errors and NLOS errors are shown collectively as environmental errors E_{env} . E_{obs} is the probability of p_{obs} , which was randomly sampled from the minimum value a_{obs} and the maximum value b_{obs} . Environmental

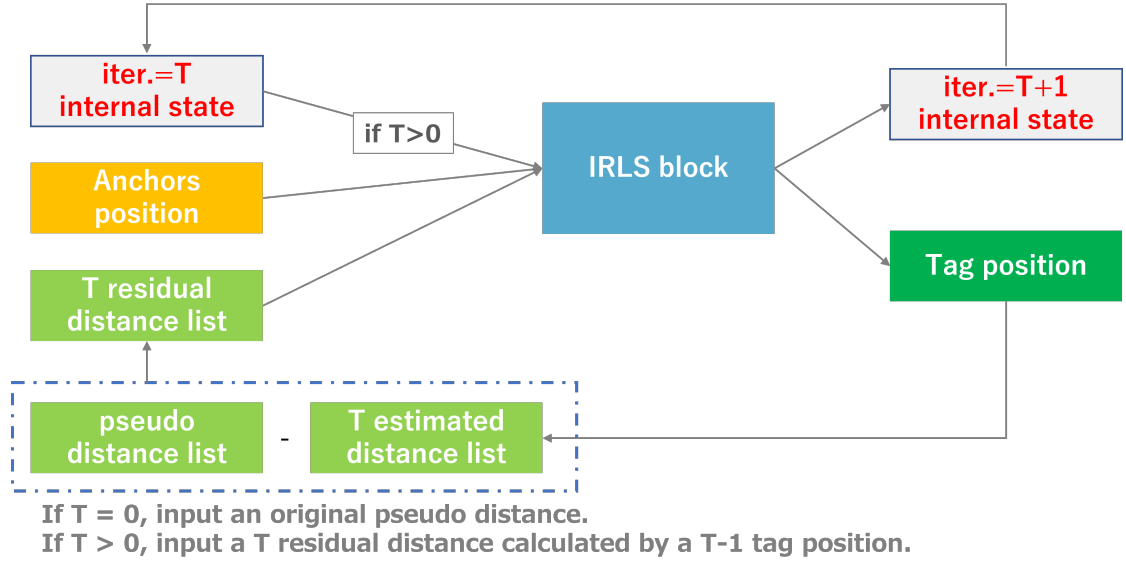


Figure 2: IRLS Net

errors E_{env} are also expressed with almost the same equation, and the absolute values of the minimum and maximum values are set to make environmental errors larger than observation errors. Figure 1 shows an overview of simulation generation. The pseudo-distance without error is the Euclidean distance between a three-dimensional anchor coordinate x_a, y_a, z_a and a tag coordinate x_t, y_t, z_t and is expressed by Equation 4. D' obtained by adding the pseudo-distance error E_{dist} to this pseudo-distance is the training data generated by the simulation used in this proposal.

$$D = \sqrt{(x_a - x_t)^2 + (y_a - y_t)^2 + (z_a - z_t)^2} \quad (4)$$

$$D' = D + E_{dist} \quad (5)$$

In this simulation, it is possible to create D' from any anchor and tag coordinates.

3.2. IRLS Net

We propose IRLS Net as a DNN model for estimating tag position. Figure 2 shows an overview of IRLS Net. IRLS Net is structured from multiple connected IRLS blocks. The input is different for the first IRLS block and for other IRLS blocks connected after the first one. In the first block, the tag position is estimated by inputting the known anchor positions and the pseudo-distances detected by signal reception. In the second and subsequent blocks, the residual of the pseudo-distance and the distance from the tag position estimated in the immediately previous block is used instead of the pseudo-distance itself to re-estimate the tag position. Multiple connected IRLS blocks are intended to perform multiple position estimations, and the residuals are passed

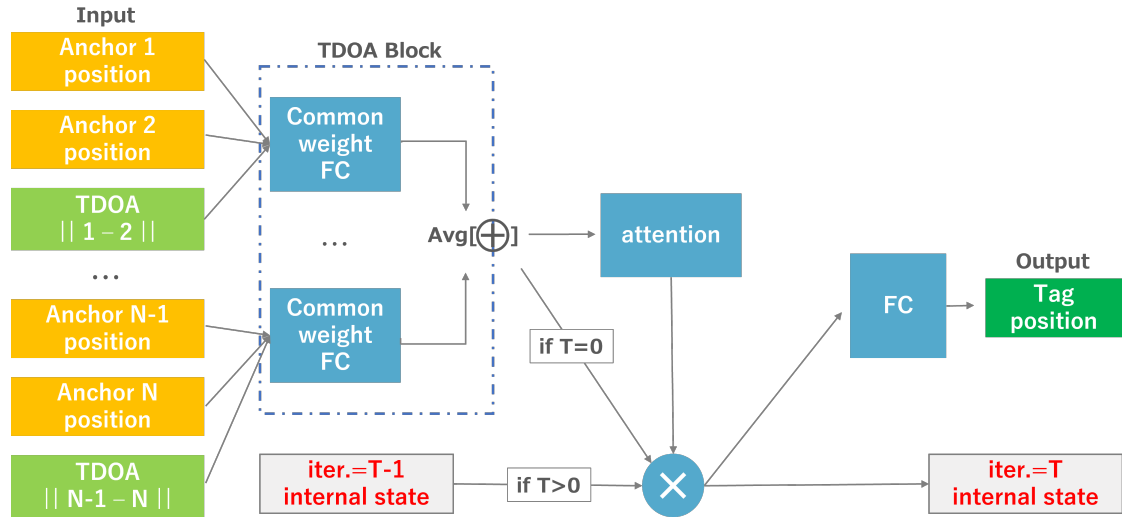


Figure 3: IRLS Block

on to the subsequent blocks so that the position estimation error is small. This model structure is inspired by IRLS, a type of gradient method.

IRLS is a method of repeatedly applying the least squares method to update the effect on estimated values so that less weight is given to outliers and observed values with large errors. Similarly, IRLS Net has multiple IRLS blocks to make iterative calculations so that residuals are small. Each IRLS block has a model structure in which learning proceeds in a way that reduces the effects of outliers and observed values with large errors. During training, the model weights are optimized with the loss function expressed by Equation 6. When there are T IRLS blocks, MSE Loss is taken for each tag estimate \hat{y}_i^t and the sum is used as the Loss function L . The later IRLS block backpropagates the MSE Loss to the previous IRLS blocks.

$$L = \sum_{t=1}^T \frac{1}{n} \sum_{i=1}^n (y_i - \hat{y}_i^t)^2 \quad (6)$$

During inference, the output of the last IRLS block is treated as the position estimation result. Each IRLS block has a different weight.

Details on IRLS blocks are shown in Figure 3. TDOA blocks within IRLS blocks are structures for model acquisition of data without synchronized time, but with variable anchor numbers and invariable order. It is assumed that time is not synchronized between the anchor and tag to be estimated. The arrival time differential is non-variable even if the anchor and tag are unsynchronized. Entering the absolute value of the arrival time differential of all anchor-tag pair combinations enables a network structure that does not require temporal syncing between anchors and tags. The common weight FC layer within TDOA blocks takes input from the positions of two anchors, while the relative distance differential of the pseudo-distance obtained from the two anchors. This process is performed for all combinations in the anchor group entered. This is entered into the shared common weight FC layer as produced for all

combinations, and average values for all combinations are sent to the following layer using average pooling. The average pooling eliminates the need for the fixed number of anchors used to estimate and for the fixed order of anchor input for passage of all combinations to the shared common weight FC layer. In the actual operations, it is not guaranteed that signals can be received from all anchors within boundaries at all times and there are often cases in which estimation must be performed from only a limited number of anchors. After a TDOA block, the system performs self-attention and estimates tag positions in all connective layers. Here, the assumption is multipath signals with data containing impact from NLOS cut for self-attention.

IRLS blocks contain multiple sequential blocks, with the second and subsequent IRLS blocks sharing the internal state of the previous IRLS block. As shown in Figure 3, the residual found from the estimated tag positions of the previous IRLS block is entered into the second and subsequent IRLS blocks, and they repeat self-attention on the internal state. This structure is expected to have equivalent effects to IRLS as a model structure that estimates tag positions using only high-certainty observed values and thus reduces the impact of error vectors like NLOS on data.

4. Experiment

An actual environment dataset was constructed using sonic wave positioning in order to verify the proposed method. We will present the experimental environment constructed and the conditions for training IRLS Net based on simulation data, as well as the results of each comparison of these results.

4.1. Real dataset collection

Extensive research has been conducted on TDOA positioning by sending and receiving sonic wave signals [19], and it has the potential for positioning without unique devices, using only consumer speakers and microphones. [20] Our experimental environment using sonic waves was also constructed for this experiment given the ease of experimental preparation. Eight consumer speakers are treated as anchors, and a microphone as a tag. Although the speakers were temporally synchronized by an audio interface, time was not synchronized between speakers and microphone. Spread spectrum codes emitted by the eight speakers and recorded by a microphone. By calculating the cross-correlation between the recorded signal and the original ones, the arrival time of them is detected. The pseudo-distance is the arrival time multiplied by the speed of sound.

Measurements were taken in four environments, including a conference room with desks and chairs, and three different living rooms with TVs, sofas and various other small items. Multiple speaker arrangements were implemented, with the microphone position moved through each arrangement in a lattice pattern to collect a total of 2950 test data.

4.2. Experimental conditions

The proposed IRLS Net learns from simulation data and performs assessments using actual environment data obtained under the conditions above. Simulation data was generated via the

Table 1
Accuracy results

Method	MAE[m]	CDF68%[m]	CDF80%[m]	CDF95%[m]
LS	0.540	0.231	0.464	3.129
WLS	0.382	0.191	0.321	2.204
No E_{dist} , IRLS Block number 1	0.633	0.503	1.004	2.238
No E_{dist} , IRLS Block number 5	0.792	0.482	1.118	3.325
E_{dist} , No attention, IRLS Block number 1	0.379	0.410	0.540	1.024
E_{dist} , IRLS Block number 1	0.336	0.341	0.484	0.997
E_{dist} , IRLS Block number 2	0.285	0.261	0.374	0.898
E_{dist} , IRLS Block number 3	0.251	0.215	0.295	0.738
E_{dist} , IRLS Block number 4	0.245	0.190	0.286	0.826
E_{dist} , IRLS Block number 5	0.230	0.180	0.262	0.748
E_{dist} , IRLS Block number 10	0.234	0.179	0.253	0.781
E_{dist} , parameter $\times 10$, IRLS Block number 1	0.291	0.258	0.375	0.890
E_{obs} , No E_{env} , IRLS Block number 5	0.550	0.453	0.745	2.348
E_{obs} , No E_{env} , IRLS Block number 10	0.679	0.472	1.123	3.231
No E_{obs} , E_{env} , IRLS Block number 5	0.280	0.244	0.336	0.826
No E_{obs} , E_{env} , IRLS Block number 10	0.257	0.232	0.320	0.747

method detailed in Section 3. In the simulation, eight anchor coordinates were determined randomly, and a tag was placed randomly within an area encompassed by the eight anchors. The number of the generated data for training is 200000. The distance between each anchor and tag is calculated at that time, and Formula 5 is given the pseudo-distance error shown in Formula 3 and used as training data. Each parameter of Formulas 1 and 2 are set as follows in this experiment. $p_{obs} = 0.5$, $a_{obs} = -0.06m$, $b_{obs} = 0.11m$, $p_{env} = 0.1$, $a_{env} = -2.15m$, $b_{env} = 2.15m$. The pseudo-distance error E_{dist} undergoes dynamic regeneration according to Formula 5 with each training iteration, and training data is updated. IRLS Net was trained under multiple conditions such as difference in the number of the IRLS blocks based on the above settings. The training was conducted in 10 epochs under each of the conditions above, and the epoch that yielded the higher accuracy was used as the assessment result.

4.3. Evaluation

Evaluation results are shown in Table 1. The MAE (Mean Absolute Error) and CDF (Cumulative Distribution Function) were applied as assessment indicators due to the distance errors between the estimated coordinates and correct coordinates. Error is shown at 68%, 80% and 95% with CDF. This research used weighted least squares (WLS) as the baseline for IRLS Net assessment. The impact of each anchor on tag position estimates is treated as a weight with WLS. The weights are recalculated using the huber function based on the residuals related to the observations for each iteration and tag position estimates are updated using the weights. The impact of the non-selected tag position estimates is expected to decline with each iteration, and more robust estimates are possible through comparison with least squares (LS) as shown in Table 1. Furthermore, the CDF for WLS and IRLS Net is shown in Figure 4. The plotted IRLS Net results have a resulting five IRLS Blocks.

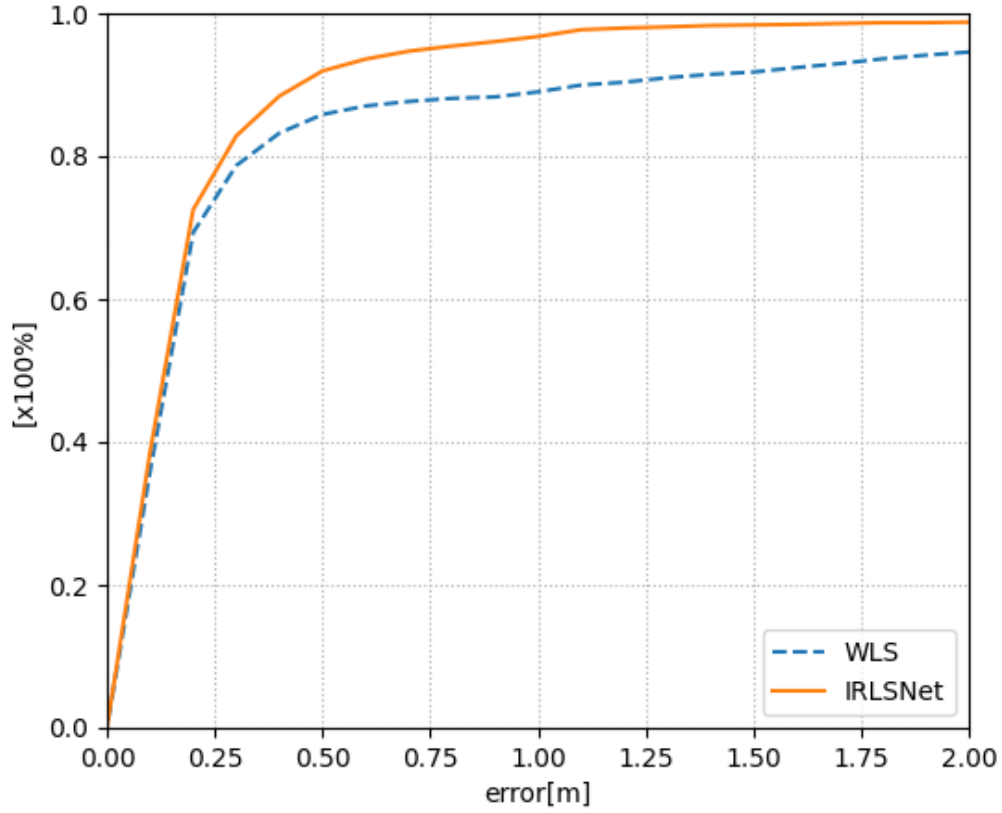


Figure 4: CDF for comparison of IRLS Net and WLS

Comparisons were performed on applying and not applying pseudo-distance error E_{dist} during training. In Table 1, results without applying a pseudo-distance error E_{dist} are shown as No E_{dist} . Under these conditions, MAE and CDF were significantly worse both when one IRLS block and five IRLS blocks were used, showing that the distribution of training data and real data used for assessment differs greatly. When the system learns without any pseudo-distance errors E_{dist} , This showed that it was completely incapable of handling real data.

The following is an examination of the effect of the attention layer. Excluding the attention layer from IRLS blocks in Figure 3 reveals a simple fully connected network from TDOA Block onward. In Table 1, the result excluding the attention layer is shown as No attention. Table 1 shows the attention layer working to reduce the impact of incorrect values, with CDF68% worsening by 0.07 m when comparing no attention versus attention (E_{dist} , IRLS Block number 1), as simple fully connected layers are not able to exclude the impact of incorrect values such as NLOS to a sufficient degree.

Next, the study confirmed the effects of multiple sequential IRLS blocks. Table 1 shows results

for sequences of 1, 2, 3, 4, 5 and 10 IRLS blocks. The results show increasing accuracy with multiple blocks in a sequence. Furthermore, experimental data showed that performance peaked with sequences of five blocks, with no major performance differences being seen between 10 IRLS Blocks and 5 IRLS Blocks. When comparing five IRLS Blocks and WLS, MAE improved by 0.152 m, CDF68% by 0.011 m, CDF80% by 0.059 m, and CDF95% by 1.456 m, with IRLS Net outperforming WLS for all indexes in Figure 4.

Table 1 shows the results for use of IRLS block layer parameters multiplied by 10 with a single block in order to verify whether the simple increase in number of network parameters contributes toward performance improvements with IRLS block sequences. Although the number of parameters is equal for a single IRLS block with 10 times the parameters and a sequence of 10 blocks, the sequence of 10 has higher performance, showing that this method is working effectively to reduce residual errors over multiple iterations.

5. Discussion

In Section 5, we will discuss the approach to pseudo-distance error E_{dist} taken in the proposed simulation. Table 1 shows assessment results when the assigned error is changed. Here, E_{obs} is the observation error from Formula 3 while E_{env} is the multipath and NLOS error components. IRLS blocks were stacked 5 and 10 times.

Although the accuracy of the results of when only the E_{obs} error is added (E_{obs} , No E_{env} , IRLS Block number 5) improved over the result of no error is added (No E_{dist} , IRLS Block number 5), when compared with WLS, this underperformed by 0.168 m by MAE, 17.7% by CDF within 15 cm, 11.5% with CDF within 30 cm and 7.5% with CDF within 45 cm. Furthermore, accuracy worsened in proportion with added IRLS blocks connected under these conditions, because the accuracy of the result of 5 IRLS Blocks is more accurate than 10 IRLS Blocks when learned with only the E_{obs} error. This result shows that the stacking of IRLS blocks was linked with reduced accuracy if training was not performed with simulation data containing adequate noise.

Results for training with only E_{env} added and for 10 IRLS blocks showed accuracy equivalent to WLS at CDF80%. This implies that learning errors equivalent to multipath and NLOS positioning produces resilience against samples containing incorrect values. In contrast, when comparing results for training with only E_{env} applied against results for E_{dist} including E_{obs} , it was clear that training with only E_{env} applied was worse by 0.041 m for CDF68% with 10 IRLS blocks. This indicates that the addition of E_{obs} contributes toward accuracy improvements for samples included in CDF68%. The impact of observation errors could not be learned adequately with just the error from E_{env} . We believe that the dominant cause of errors in the sample, which were measurement errors with low impact from multipath and NLOS, could not be fully excluded. When E_{obs} was added to impart observation errors to the training data, performance improved for these cases.

Based on these discussions, the inclusion of both the observation error E_{obs} and the environmental error E_{env} due to multipath and NLOS effects in the training data showed that our method was applicable to actual environment data with high accuracy. These pseudo-distance errors can be generated extremely easily without an actual environment or 3D map, allowing for creation of training data with pseudo-distance errors in great quantities. When deep network

structure like IRLS Net is used, it is easy to overfit with limited data. computational costs for this ray tracing-free simulation method are lower than those for ray tracing, and it is possible to generate training data in real time. Training with massive quantities of generated data confirmed that this could be generalized to actual environment data not included in training data while avoiding over-fitting.

6. Conclusion

This paper proposed IRLS Net as a new DNN structure and training the model using ray tracing-free simulation to resolve measurement precision loss issues encountered due to multipath and NLOS. An experimental environment was constructed using speakers and a microphone for sonic wave positioning, and actual environmental data was collected for evaluation of the proposed method. This ray tracing-free simulation method works by assigning multipath, NLOS error for pseudo-distances, and does not require precise simulation of factors like indoor signal reverberation or indoor 3D map creation. The method can easily generate large amounts of simulation data, and the IRLS Net trained with it have shown high accuracy even with actual data collected in a variety of environments. The IRLS Net has a model structure inspired by IRLS, and achieves high-precision positioning with reduced impact from observed values from multiple IRLS blocks with incorrect values. As a result, the proposed method demonstrated superior results as compared with the baseline TDOA positioning method, WLS. The proposed method can be adopted for general positioning technologies such as UWB.

References

- [1] K. Ho, Y. Chan, Geolocation of a known altitude object from tdoa and fdoa measurements, *IEEE Transactions on Aerospace and Electronic Systems* 33 (1997) 770–783. doi:10.1109/7.599239.
- [2] H. Jiang, J. Xu, Z. Li, Nlos mitigation method for tdoa measurement, in: 2010 Sixth International Conference on Intelligent Information Hiding and Multimedia Signal Processing, 2010, pp. 196–199. doi:10.1109/IIHMSP.2010.56.
- [3] X.-W. Chang, Y. Guo, Huber’s m-estimation in relative gps positioning: computational aspects, *Journal of Geodesy* 79 (2005) 351–362.
- [4] J. Park, S. Nam, H. Choi, Y. Ko, Y.-B. Ko, Improving deep learning-based uwb los/nlos identification with transfer learning: An empirical approach, *Electronics* 9 (2020) 1714.
- [5] A. Olejniczak, O. Blaszkievicz, K. K. Cwalina, P. Rajchowski, J. Sadowski, Deep learning approach for los and nlos identification in the indoor environment, in: 2020 Baltic URSI Symposium (URSI), IEEE, 2020, pp. 104–107.
- [6] L. Flueratoru, E. S. Lohan, D. Niculescu, Self-learning detection and mitigation of non-line-of-sight measurements in ultra-wideband localization, in: 2021 International Conference on Indoor Positioning and Indoor Navigation (IPIN), IEEE, 2021, pp. 1–8.
- [7] A. V. Kanhere, S. Gupta, A. Shetty, G. Gao, Improving gnss positioning using neural-network-based corrections, *NAVIGATION: Journal of the Institute of Navigation* 69 (2022).
- [8] G. Félix, M. Siller, E. N. Alvarez, A fingerprinting indoor localization algorithm based deep

- learning, in: 2016 eighth international conference on ubiquitous and future networks (ICUFN), IEEE, 2016, pp. 1006–1011.
- [9] M. Nabati, S. A. Ghorashi, A real-time fingerprint-based indoor positioning using deep learning and preceding states, *Expert Systems with Applications* 213 (2023) 118889.
- [10] A. Poulose, D. S. Han, Uwb indoor localization using deep learning lstm networks, *Applied Sciences* 10 (2020) 6290.
- [11] Y.-M. Lu, J.-P. Sheu, Y.-C. Kuo, Deep learning for ultra-wideband indoor positioning, in: 2021 IEEE 32nd Annual International Symposium on Personal, Indoor and Mobile Radio Communications (PIMRC), IEEE, 2021, pp. 1260–1266.
- [12] X. Wang, X. Wang, S. Mao, Resloc: Deep residual sharing learning for indoor localization with csi tensors, in: 2017 IEEE 28th Annual International Symposium on Personal, Indoor, and Mobile Radio Communications (PIMRC), IEEE Press, 2017, p. 1–6. URL: <https://doi.org/10.1109/PIMRC.2017.8292236>. doi:10.1109/PIMRC.2017.8292236.
- [13] R. S. Sinha, S.-M. Lee, M. Rim, S.-H. Hwang, Data augmentation schemes for deep learning in an indoor positioning application, *Electronics* 8 (2019). URL: <https://www.mdpi.com/2079-9292/8/5/554>. doi:10.3390/electronics8050554.
- [14] S. Yean, P. Somani, B.-S. Lee, H. L. Oh, Gan+: Data augmentation method using generative adversarial networks and dirichlet for indoor localisation., in: IPIN-WiP, 2021.
- [15] P. Pertilä, M. Parviainen, V. Myllylä, A. Huttunen, P. Jarske, Time difference of arrival estimation with deep learning – from acoustic simulations to recorded data, in: 2020 IEEE 22nd International Workshop on Multimedia Signal Processing (MMSP), 2020, pp. 1–6. doi:10.1109/MMSP48831.2020.9287131.
- [16] L.-T. Hsu, Gnss multipath detection using a machine learning approach, in: 2017 IEEE 20th International Conference on Intelligent Transportation Systems (ITSC), IEEE, 2017, pp. 1–6.
- [17] M. N. de Sousa, R. S. Thomä, Enhancement of localization systems in nlos urban scenario with multipath ray tracing fingerprints and machine learning, *Sensors* 18 (2018) 4073.
- [18] M. Stahlke, T. Feigl, M. H. C. García, R. A. Stirling-Gallacher, J. Seitz, C. Mutschler, Transfer learning to adapt 5g ai-based fingerprint localization across environments, in: 2022 IEEE 95th Vehicular Technology Conference:(VTC2022-Spring), IEEE, 2022, pp. 1–5.
- [19] H. Murakami, Y. Kandori, T. Suzaki, M. Nakamura, H. Watanabe, H. Hashizume, M. Sugimoto, NI-beep: A ranging system between multiple smartphones using acoustic sensing in nlos environments, in: 2021 International Conference on Indoor Positioning and Indoor Navigation (IPIN), IEEE, 2021, pp. 1–8.
- [20] Y. Zhuang, Y. Wang, Y. Yan, X. Xu, Y. Shi, Reflectrack: Enabling 3d acoustic position tracking using commodity dual-microphone smartphones, in: The 34th Annual ACM Symposium on User Interface Software and Technology, 2021, pp. 1050–1062.